

# Rheology of Soft Materials

Daniel T.N. Chen,<sup>1</sup> Qi Wen,<sup>2</sup> Paul A. Janmey,<sup>2</sup>  
John C. Crocker,<sup>3</sup> and Arjun G. Yodh<sup>1,\*</sup>

<sup>1</sup>Department of Physics and Astronomy, University of Pennsylvania, Philadelphia, Pennsylvania 19104; email: danieltn@physics.upenn.edu; yodh@physics.upenn.edu

<sup>2</sup>Departments of Physiology, Physics, and Bioengineering, Institute for Medicine and Engineering, University of Pennsylvania, Philadelphia, Pennsylvania 19104; email: wenqi@mail.med.upenn.edu; janmey@mail.med.upenn.edu

<sup>3</sup>Department of Chemical and Biomolecular Engineering, University of Pennsylvania, Philadelphia, Pennsylvania; email: jcrocker@seas.upenn.edu

Annu. Rev. Condens. Matter Phys. 2010. 1:301–22

First published online as a Review in Advance on May 24, 2010

The *Annual Review of Condensed Matter Physics* is online at [conmatphys.annualreviews.org](http://conmatphys.annualreviews.org)

This article's doi:  
10.1146/annurev-conmatphys-070909-104120

Copyright © 2010 by Annual Reviews.  
All rights reserved

1947-5454/10/0810-0301\$20.00

\*Corresponding author

## Key Words

viscoelasticity, nonlinear rheology, microrheology, polymer network, colloidal glass

## Abstract

Research on soft materials, including colloidal suspensions, glasses, pastes, emulsions, foams, polymer networks, liquid crystals, granular materials, and cells, has captured the interest of scientists and engineers in fields ranging from physics and chemical engineering to materials science and cell biology. Recent advances in rheological methods to probe mechanical responses of these complex media have been instrumental for producing new understanding of soft matter and for generating novel technological applications. This review surveys these technical developments and current work in the field, with partial aim to illustrate open questions for future research.

**Elastic:** property of a material to deform to a defined extent in response to a force and then return to its original state when the force is removed

**Stress:** force per unit area;  $\sigma = F/A$ ; SI unit is  $\text{N/m}^2$

**Viscoelastic:** property of soft materials to exhibit both elastic and viscous responses in a frequency-dependent manner

**Strain:** unitless parameter quantifying the extent of deformation after application of stress

**Viscosity:** measure of resistance of a fluid to shear stress;  $\eta = \sigma / \dot{\gamma}$ , where  $\dot{\gamma}$  is the rate of strain

**Strain stiffening:** rheological response of a material in which the stress increases with increasing strain, often used to describe polymer networks

**(Non)-linear elasticity:** Young's or shear modulus that (does not change) changes with strain

## 1. INTRODUCTION

Rheology is the study of how materials deform when forces are applied to them. The foundations of rheology rest on theories describing ideal materials. One example is Robert Hooke's description of ideal elastic behavior being a solid wherein the extension of the material is proportional to the load imposed on it, and which recovers to its initial state when the load is removed. By contrast, Isaac Newton's theory describing ideal liquids states that an irreversible flow will persist as long as a stress is applied, with flow rate proportional to stress.

Real materials, and especially soft materials, are neither ideal solids nor ideal liquids. Real soft materials exhibit both elastic and viscous responses and are therefore called viscoelastic. The internal structures of soft solids and complex fluids composed of colloidal particles, filamentous polymers, and other supra-molecular arrangements lead to complicated deformations in response to mechanical stress. As a result, the relations between stress and strain are not simply defined by elastic and viscous constants; rather, they are functions of time, direction, and extent of deformation. The goal of rheological experiments is to quantify dynamic viscoelasticity over as wide a range of time and deformation scales as possible, and ultimately to relate these viscoelastic properties to material structure. Many open questions remain about how to relate structure to viscoelastic response. This review focuses on recent progress in soft material rheology, with particular orientation toward new experimental techniques suitable for studies of colloids, glasses, filamentous networks, granular materials, emulsions, and cells.

## 2. OVERVIEW OF TECHNIQUES

### 2.1. Rheology

Rheometers generally measure two quantities: stress, the amount of force per unit area applied to the sample; and strain, the dimensionless degree to which the material deforms. Material properties, quantified as elastic moduli for solids or viscosity for liquids, are calculated from the ratio of stress to strain or strain rate, respectively. To characterize fully the viscoelastic properties of complex soft materials, the relation of stress to strain must be measured over a wide range of strains, strain rates, and time scales (**Figure 1**). Recent advances in rheological methods have been motivated, in part, by attempts to measure delicate samples with complex time-dependent responses at the micron scale, and microrheological methods, in particular, have even been extended for use in live cells. Additional experimental and theoretical progress has been made on systems far from equilibrium, e.g., systems in which nonthermal sources of energy drive fluctuations and rheological responses.

**2.1.1. Nonlinear measurements.** The useful properties of soft materials are often related to their responses at large strains. This is especially true for biological tissues such as blood vessels, lung, or muscle that are stretched tens of percent during normal function, and even more during injury. A common feature of soft tissues is their nonlinear viscoelastic response, which is evident as a stiffening with increasing strain, termed strain stiffening.

Even networks of purified biopolymers such as actin, fibrin, or collagen exhibit nonlinear elasticity at strains where rubber-like elastomers or hydrogels made from

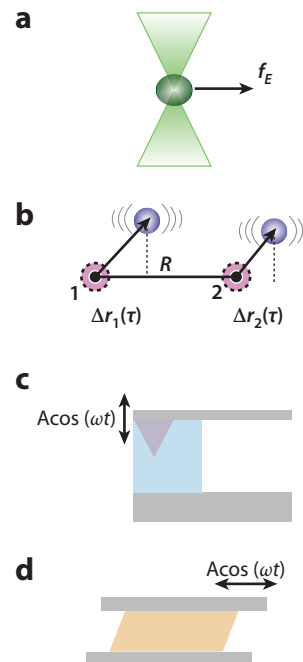
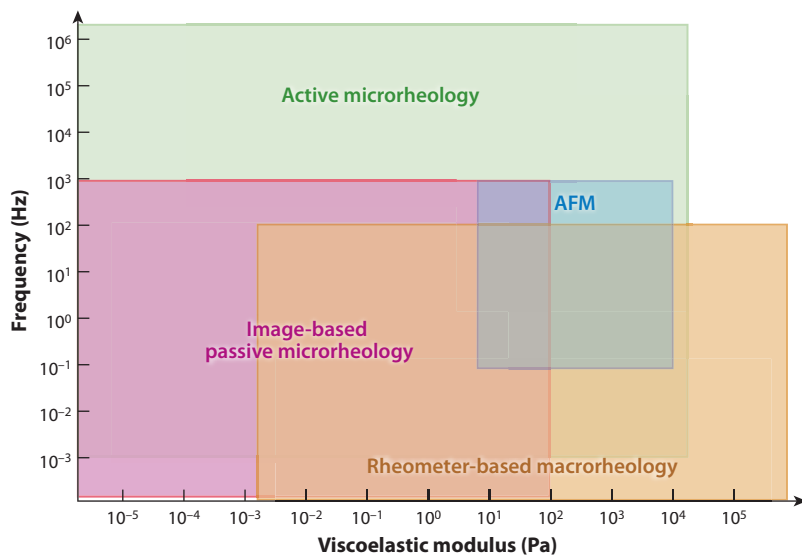


**Figure 1**

Rheological techniques employed to probe soft materials. Graph: typical frequency and viscoelastic modulus range of techniques. (Note: contours show minimum/maximum ranges of the techniques). Schematic illustrations of (a) active microrheology using optical tweezers to force probe particle. (b) Passive two-point microrheology using image-based particle tracking. (c) Dynamic material deformation using atomic force microscopy (AFM). (d) Oscillatory macrorheology.

cross-linked flexible polymers maintain a linear elastic response (1–4). An example of this contrast in the storage modulus ( $G'$ ) of biopolymer gels and flexible polymer gels such as polyacrylamide is shown in **Figure 2**. Here, the moduli of different cross-linked networks are compared at increasing strains. The nonlinear responses of semiflexible or rod-like polymers present challenges for experimental methods, as well as for new theories.

Two approaches have been used to improve the analysis of soft strain-stiffening materials. If the material exhibits very little creep, a constant stress can be imposed to produce a given amount of strain, and then a small incremental oscillatory stress is superimposed. This approach results in a nearly sinusoidal strain response (4, 5). In this case, the so-called incremental measurement reflects the stiffness of the sample in the deformed state (6). A second approach plots the instantaneous stress and strain data from each oscillation on orthogonal axes, using a method termed large amplitude oscillatory shear analysis (7). The storage and loss moduli ( $G''$ ) can then be calculated from the slopes and differences between the stress magnitudes at a given strain from the ascending and descending part of the sinusoid.

**2.1.2. Rheo-optical measurements.** Measurement of stress or strain alone is often not enough to fully characterize the detailed deformations that give rise to the macroscopic response of a material. Frequently, soft materials sheared at large amplitudes can undergo

**Storage modulus ( $G'$ ):**

measure of energy stored during a strain cycle; the real part of the complex shear modulus  $G^*(\omega) = G'(\omega) + iG''(\omega)$ . Also termed the elastic modulus.

**Loss modulus ( $G''$ ):**

measure of energy lost during a strain cycle; the imaginary part of the complex shear modulus  $G^*(\omega) = G'(\omega) + iG''(\omega)$ ; also termed the viscous modulus

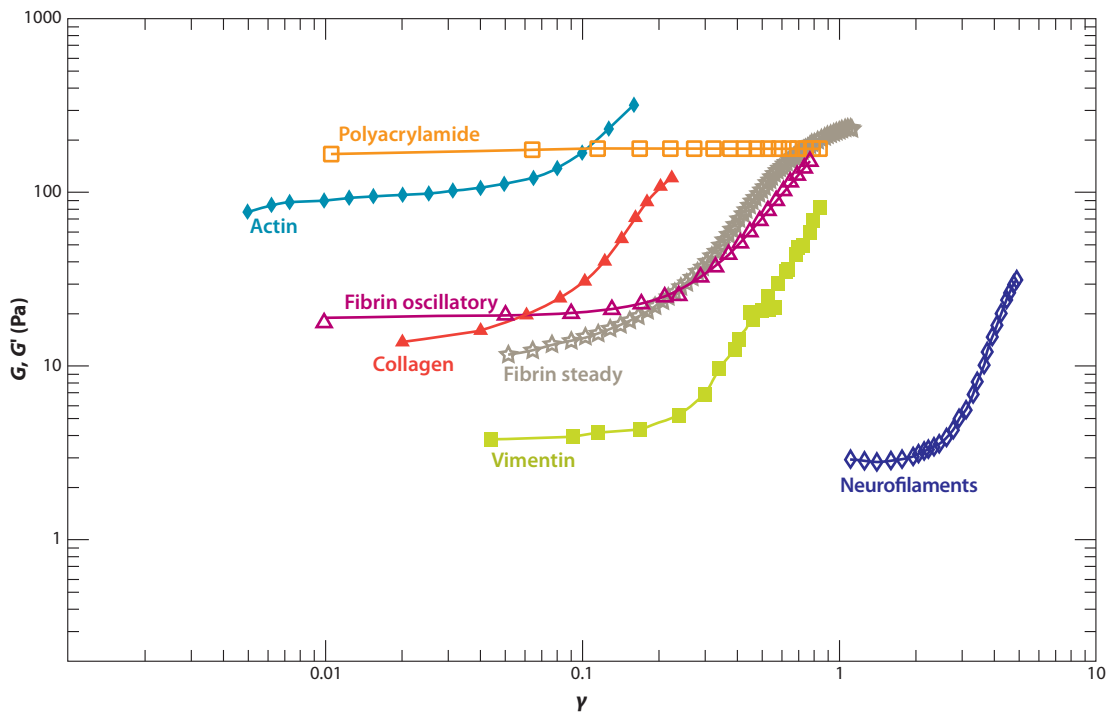


**Figure 2**

Dynamic shear storage moduli measured at different strain amplitudes for a series of cross-linked biopolymer networks. The real part,  $G'$ , of the storage modulus reduces to the shear modulus  $G$  at zero frequency. Data shown are  $G'$  (at  $10 \text{ rad s}^{-1}$ ) values for F-actin, fibrin, collagen, vimentin, and polyacrylamide; and shear modulus  $G$  for fibrin and neurofilaments, plotted as a function of the dimensionless strain  $\gamma$ . Strain stiffening behavior is observed in the cross-linked biopolymer networks. Adapted from Reference 2. Reprinted with permission.

**Shear banding:**

formation of regions in a material undergoing shear strain in which part of the sample is fluidized while other parts remain solid

structural transitions such as ordering, crystallization, or shear banding, and these transitions confound interpretation in the absence of a model that anticipates their onset. In shear banding (8–10), for example, the sheared material separates into regions characterized by different viscosities. As a result, the same measured stress value can result from two or more applied strain rates. Experimentally, this complication can be accounted for by applying shear deformation concurrent with in situ characterization of the material's microstructure. A variety of schemes are employed to accomplish this structural characterization. Broadly speaking, rheo-optical characterization falls under two categories depending on whether the information is obtained via real-space imaging or via scattering in reciprocal space. Real-space techniques involve the use of fluorescence microscopy (11, 12) or magnetic resonance imaging (13, 14) to image through a shear cell (15) or rheometer (16). Scattering techniques typically involve measuring changes in 2D scattering patterns under flow using light, X-rays, or neutrons. The presence of ordering in the sheared material typically results in the appearance of a distinct peak at the inverse wavelength of the ordering in the scattering pattern. For more detailed reviews of scattering-based rheo-optical measurements see References 17 and 18.

## 2.2. Microrheology

Situations in which traditional rheometers are difficult to use, such as when materials are available in very low quantities, have spurred the development of microrheological techniques. These techniques, in turn, have augmented the scope of materials that can be rheologically probed.

**2.2.1. Methods and instruments.** Microrheology describes a collection of techniques to quantify the shear moduli of very small samples or objects such as cells. The mechanical properties of cells were estimated nearly a century ago by watching the motion of magnetic particles ingested by cells (19, 20). Since then, a number of methods based on particle tracking have been developed. These techniques can be classified according to whether they rely on the motion of a probe in response to an applied force (termed active microrheology) or rather, on the Brownian motion of the material or probe (termed passive microrheology). In the former case, the principle is the same as a macroscopic rheometer: An oscillatory stress (or strain) is applied and the resulting strain (or stress) is measured, and then the complex ratio is computed. Or, alternatively, measurements can be performed in a step strain (or stress) manner: The creep modulus is computed and then converted to dynamic shear moduli by standard integral transforms.

Passive microrheology uses the fluctuation-dissipation theorem (FDT) to relate the spectrum of fluctuating forces in a material proportionally to the loss (viscous) modulus of the material. By invoking the FDT, one can employ a generalized Stokes-Einstein relation that relates the Brownian mean-squared displacement (MSD) of the probe particle to the dynamic shear modulus by simple integral transforms (21, 22). Compared to active methods, passive methods are generally better suited to softer materials, are straightforward to calibrate, and can be adapted to a wide range of instruments. All that is required is a method of measuring particle or probe MSD, such as laser-deflection tracking (22, 23), optical tweezers (24, 25), diffusing wave spectroscopy (26, 27), dynamic light scattering (28, 29), image-based tracking (30–32), optical interferometry (33), or atomic force microscopy (AFM) noise analysis (34).

In contrast, active methods require more complex instrumentation than passive methods, but they are ultimately more versatile, permitting measurements of harder samples and nonlinear rheological behavior (35–37). Early work relied on micropipette aspiration (38), later refined to include time-dependent effects (39, 40). The early magnetic particle research was refined into a quantitative creep method (41) as well as oscillatory rotational approaches (42), termed magnetic twisting cytometry (MTC) (43, 44). Oscillatory optical tweezers can be used for active measurements (45–47), as well as passive ones. Much recent work has been performed with AFM (48, 49).

**2.2.2. Two-point microrheology.** The proper interpretation of all microrheology methods, however, relies on knowing the boundary conditions at the probe/soft material interface and the shape of the strain field, which can be poorly controlled compared to a macroscopic rheometer. Pioneering early work in cells examined the motion of nonmagnetic tracers near driven magnetic particles to map out the deformation field (42, 50) and found significant deviations from continuum behavior. Two-point microrheology (TPM) (31) uses the correlated motion of two well-separated tracers to measure the rheological response, with the effect that the measurement becomes insensitive to tracer

---

**FDT:** fluctuation-dissipation theorem

**MSD:** mean-square displacement

**Shear modulus:** constant describing a material's resistance to deformation as given by the ratio of shear stress to shear strain,  $G = \sigma / \gamma$

**MTC:** magnetic twisting cytometry

**TPM:** two-point microrheology

---

---

**(Non)-Newtonian:** class of fluids having the defining property that their viscosity is (dependent on) independent of shear rate.

---

boundary conditions (51, 52). This robustness can be turned around to study the nature of the probes' boundary conditions with the matrix (24, 32) and even inertial effects (53). Whereas much early TPM work used an image-based passive approach, it has been adapted to dynamic light scattering (54) and optical tweezer-based instruments (25, 55).

**2.2.3. Force spectroscopy of active materials.** Finally, in the interesting case where the sample contains endogenous force generators, a combination of both passive and active microrheology data provides a method for quantifying the internal forces. Early researchers noted that the MSDs of embedded tracers in cells had a functional form incompatible with Brownian motion (56, 57); such motions could be modeled as a viscoelastic material driven by fluctuating stresses having a simple power-law form (56) and were subsequently confirmed by MTC (58) and two-point measurements in cells (59), with the latter also showing that two-point techniques do not require FDT. Similar measurements on non-Brownian stresses were made in bacterial baths (47) and in a cytoskeleton model of reconstituted biopolymers and motors (60); the latter compares favorably to measurements of living cells (61). A recent study combining active and passive measurements on the same cell-adhered probes reported non-Brownian stresses having the same frequency dependence as expected from the FDT, but with an amplitude several times larger (62), which may be interpreted in terms of an effective granular temperature.

### 3. SOFT MATERIALS

#### 3.1. Colloidal Suspensions and Glasses

Full understanding of even a monodisperse hard-sphere colloidal suspension's rheology requires detailed consideration of the interplay between Brownian, conservative interparticle, and hydrodynamic forces. The central quantity of interest for determining colloid rheology is the spatial distribution of the particles, termed the microstructure, which is set by the balance of forces in equilibrium. Under imposed flow, the ability of the microstructure to rearrange to accommodate flow and interparticle forces determines its macroscopic rheological response. The many-body, shear-history-dependent nature of the microstructure renders the prediction of the suspension's dynamics and rheology highly nontrivial. Driven in part by their technological importance in many staple industrial products such as paints and food additives, the study of colloidal suspensions continues. Currently, colloidal suspensions are also the test bed for ideas in soft matter, e.g., their study is leading to new insights about deep problems in the field, such as the glass transition (63).

**3.1.1. Influence of particle volume fraction.** The addition of colloidal particles to a Newtonian fluid causes the viscosity of the medium to increase. This effect is essentially due to particles being rigid objects that can move and rotate, but not shear with the suspending fluid. As such, they exert an additional stress in the form of quadrupolar disturbances on the fluid. In the very dilute limit ( $\phi < .02$ ), where each particle is far enough away from the other particles (and thus do not interact hydrodynamically), Einstein (64) derived the relationship between the zero-shear viscosity and volume fraction:  $\eta = \eta_0(1 + \frac{5}{2}\phi)$ . As  $\phi$  increases, the displacement of a particle causes a displacement of the incompressible suspending fluid, which in turn gives rise to long-range and many-body hydrodynamic forces that couple neighboring particles. In the dilute limit ( $\phi < 0.1$ ), consideration of pairwise hydrodynamic interactions is sufficient and leads to  $O(\phi^2)$  corrections to

Einstein's result (65). For a review of more recent work on non-Newtonian rheology in colloidal suspensions, see Reference 66.

Under the right conditions, colloidal suspensions can crystallize. However, most often colloidal suspensions undergo a glass transition as particle density is increased to  $\phi \sim 0.6$ . Near this colloidal glass transition, volume fraction plays a role analogous to temperature in molecular liquids. Broadly speaking, an increase in the particle volume fraction causes crowding. Crowding, in turn, leads to dynamical arrest: Thermal energy is insufficient to drive the configurational rearrangements necessary for equilibration. As a result, the system becomes trapped in metastable states, characterized by liquid-like structural order. Colloidal glasses share many qualitative similarities to granular materials that have led to the conjecture that they can both be described within a common theoretical framework known as jamming (67, 68). Accompanying the dynamical arrest are a concomitant divergence of the suspension viscosity and development of a finite yield stress ( $\sigma_y$ ), below which there is no flow.

The low-shear rheology of noncrystalline, hard-sphere colloidal suspensions of volume fraction up to  $\phi \approx 0.6$  has been extensively studied (69–71). In linear oscillatory measurements (69), it was found that for  $\phi \leq 0.5$ , the loss modulus ( $G''$ ) dominates the response for all frequencies; as  $\phi$  increases, both moduli increase, with the storage modulus  $G'$  increasing faster than  $G''$  and eventually dominating for lower frequencies. Near  $\phi \sim 0.58$ , the low-frequency  $G'$  exhibits a nearly frequency-independent plateau, i.e.,  $G'(\phi) \sim G_0 = f(\phi) * k_B T / a^3$ , where  $a$  is the particle radius and  $f(\phi)$  denotes a function of  $\phi$  (71). This low-frequency behavior is a direct consequence of particles being trapped by their neighbors and the stress in the suspension being unable to relax on the longest time scale of the measurement. This linear viscoelasticity is quite generic; most jammed systems (e.g., entangled polymer solutions, weak polymeric gels, concentrated emulsions) exhibit similar trends in their respective moduli when densities and shear rates are such that the relaxation time is longer than the measurement time scale.

Viscometry has been used to measure the divergence of viscosity in noncrystalline hard-sphere suspensions as the glass transition is approached (70). These measurements, spanning several orders of magnitude and taken together with recent measurements of the structural relaxation time  $\tau_\alpha$  from light scattering (72), suggest that the viscosity divergence occurs at higher density than predictions of mode-coupling theory (MCT) (73). MCT predicts a power-law divergence of the viscosity at  $\phi \approx 0.58$ . The current consensus from experiments appears to be that the viscosity divergence is better captured by a Vogel-Fulcher-Tammann exponential form  $\eta = \eta_0 \exp(A\phi/(\phi_0 - \phi))$  with the critical volume fraction  $\phi_0$  closer to random close packing  $\phi_{rcp} = 0.64$ , in accord with expectations based on free-volume theory (74).

**3.1.2. Influence of shear rate.** Shear rate has profound consequences on the rheology of colloidal suspensions. Shear rate is parameterized by the Peclet number (Pe), which is the ratio of the applied shear rate  $\dot{\gamma}$  to the inverse of the Brownian relaxation time  $D/a^2$  of the colloidal suspension:  $Pe = \dot{\gamma} a^2 / D$ . Pe is a measure of how far the suspension's microstructure is driven from equilibrium. At low Pe, Brownian forces are able to restore shear-induced perturbations to the equilibrium microstructure on the time scale of the shear flow. As Pe increases, Brownian motion is insufficient to restore the microstructure and, as a result, interparticle hydrodynamic forces dominate the suspension's rheological response. At  $Pe \sim 1$ , particles become ordered by the flow and can organize into layers

---

**Peclet Number (Pe):**  
dimensionless ratio of  
the applied shear rate  
to inverse Brownian  
relaxation time  
quantifying relative  
importance of  
advection to diffusion:  
 $Pe = \dot{\gamma} a^2 / D$

---

**Shear thickening (thinning):**

Non-Newtonian rheological behavior of a material in which the stress increases (decreases) with increasing shear rate

that are able to flow with less resistance, reducing the suspension’s viscosity. This effect, known as shear thinning, is a generic feature of colloidal suspensions at intermediate  $Pe$ . Shear thinning is defined by the behavior that, at high shear rate,  $\dot{\gamma}$ , the shear stress  $\sigma \propto \dot{\gamma}^n$  with  $n < 1$ ; therefore, the apparent viscosity  $\eta \equiv \sigma/\dot{\gamma}$  decreases as the shear rate increases. This effect covers a wide range of materials that can become Newtonian ( $n = 1$ ) at low shear rates or have a yield stress. Empirically, colloidal glasses and most other soft glassy materials (SGM) have a flow behavior that is well described by the Herschel-Bulkley relation:  $\sigma = \sigma_y + C\dot{\gamma}^n$ , where  $\sigma_y$  is the yield stress below which there is no flow and  $n \leq 1$ .  $\sigma_y$  depends on volume fraction and  $n$  depends on constitutive properties of the material.

As  $Pe$  further increases, hydrodynamic interactions can induce particles to orbit one another, destabilizing their ordered, layered flow structure. In this case, the increased number of collisions in the disordered state leads to a regime of shear thickening, wherein the viscosity dramatically increases. The particles organize into hydroclusters, as depicted in Figure 3. The shear thickening transition is believed to result from particular

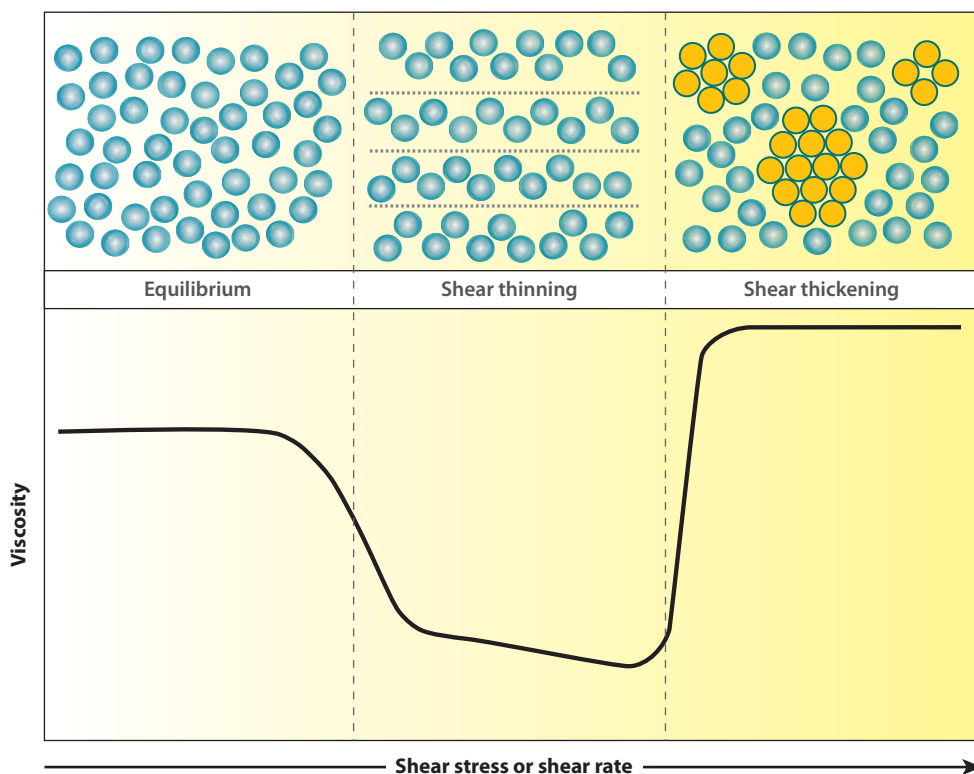


**Figure 3**

Relationship between microstructure and viscosity of shear thinning-shear thickening transition in hard-sphere colloidal suspensions. In equilibrium, random collisions among particles (*blue spheres*) make them naturally resistant to flow. However, as the shear stress or, equivalently, the shear rate increases (*increasing yellow gradient fill*), particles become organized in the flow, which lowers their viscosity. At yet higher shear rates, hydrodynamic interactions between particles dominate over stochastic ones, a change that spawns hydroclusters (*orange spheres*)—transient fluctuations in particle concentration. The difficulty of particles flowing around each other in a strong flow leads to a higher rate of energy dissipation and an abrupt increase in viscosity. Based on Figure 2 of Reference 76.

hydrodynamic forces known as lubrication forces that arise whenever two surfaces, separated by a fluid, move relative to one another in close proximity. Lubrication forces are short ranged and divergent at contact; thus, they can only be observed at high  $Pe$  because normal Brownian and repulsive interparticle forces conspire to prevent such close approach. Wagner and coworkers have carefully studied the particle size, surface chemistry, concentration, and  $Pe$  dependencies for this novel reversible shear thickening effect (75). More details are found in References 17 and 76. Currently, these materials are being developed as the basis for soft body armor.

---

**Aging:** property of a material wherein its measured rheological response depends on sample lifetime

---

**3.1.3. Active particle suspensions.** A frontier research area in colloidal suspension rheology concerns a new class of soft matter termed active suspensions. Active particle suspensions arise when the motion of constituent particles is driven by nonthermal internal energy sources. A canonical example of this system is a suspension of swimming microorganisms in which the particles are actively consuming chemical energy and dissipating it into the medium through their motion. In such a scenario, the dynamics of the particles are no longer constrained by the FDT to the medium's rheological linear response. A recent theory has predicted that the medium's viscosity can thus be altered by active forcing (77). The viscosity can be either enhanced or suppressed, depending on the symmetry of the forcing mechanism. This prediction is somewhat counter-intuitive, given that passive spherical particles at low-to-moderate  $Pe$  will always increase stress in suspension, resulting in viscosity enhancement. Recent passive and active microrheological measurements of passive tracers in bacterial suspensions have observed clear violation of the FDT at low bacterial densities ( $\phi \sim .001$ ) (47). A continuum theory elucidating the interplay between active stress, orientational dynamics, and hydrodynamics has been developed and used to rationalize microrheological measurements of passive tracer dynamics in active suspensions (78). There have been many observations of self-organized collective motion in the form of jets and vortices in concentrated bacterial suspensions (79, 80), and it is worthwhile to consider what role, if any, this collective-motion-induced ordering plays in modification of system rheology, i.e., whether such ordering produces viscosity reduction akin to ordering in sheared colloidal suspensions at moderate  $Pe$ . Indeed, recent work has interpreted the coherence lifetime of vortices as a measure of viscosity reduction in active bacterial suspensions (81).

**3.1.4. Summary and future directions.** Many researchers are exploring the structural and dynamical transitions in colloidal suspensions that accompany the glass transition. Several such studies have focused on the phenomena of dynamical heterogeneities near the glass transition wherein groups of particles move in a coordinated fashion with displacements far exceeding that expected for pure diffusion (82–84). Particles within these dynamically heterogeneous regions are sometimes qualitatively described as moving in a string-like manner, and the participation fraction and spatio-temporal extent of these motions often exhibit scaling near the glass transition critical volume fraction. Relatively unexplored are the rheological transitions that accompany the glass transition, and even less well understood are the rheological impacts of dynamical heterogeneities, if any, and their possible connection to theoretical frameworks, such as shear transformation zones (85). Experiments that directly observe correlations between stress relaxation and dynamical heterogeneity in a sheared colloidal glass have recently appeared (86, 87). In a related vein, studies of particle dynamics in aging glasses have been carried out (84, 88). The aim of these

**(Non)-universal exponents:** exponents characterizing rheological responses having values that (do not) depend on details of sample formulation

**Rejuvenation:** property of aging materials wherein rheological response can be reset to an earlier state via external shear or internal rearrangement processes

studies has been to reveal which particle configurations give rise to aging behavior, in essence linking structure to dynamics. However, rheological studies in which aging glasses have been simultaneously imaged under weak (perturbative) shear are scarce. Such studies may unveil the subtle, as-yet-unknown, microscopic mechanisms of aging in glasses. Technological advances in rheo-optical methods should provide opportunities to achieve a comprehensive characterization of these phenomena in the near future.

### 3.2. Soft Glassy Materials

SGM encompass a host of new media including pastes (89), foams (90), emulsions (91, 92), colloids (69, 93), clay suspensions (94), star polymer gels (95), and multilamellar vesicle gels (96). These materials share a set of unusual rheological properties (97), whose physical origin remains mysterious despite considerable research attention. SGM generally appear as very soft solids, yet flow readily above a yield stress ( $\sigma_Y$ ) (98, 99). Rheometric measurements report behavior that can be described by the Herschel-Bulkley relation. Typically, the exponent  $n < 1$ , making them shear thinning or pseudoplastic materials. As such, their flow profiles are often complex (14, 100, 101), displaying wall slip and shear banding behavior (102, 103).

Linear rheology measurements on these materials show a predominantly elastic response having an apparent power-law form:  $G'(\omega) \sim \omega^\beta$ , with a small exponent  $0 < \beta < 0.3$ , over a few decades of frequency (69, 91). Moreover, the loss modulus ( $G''$ ) is anomalously large at low frequencies, when compared to conventional, elastic soft materials: typically  $G''(\omega)/G'(\omega) \sim O(0.1)$ . A notable feature of the power-law rheology exponents,  $\beta$ , is that they vary among different materials and that they can vary continuously (though typically rather weakly) for a single material type, depending on its formulation (e.g., solid fraction). Such nonuniversal exponents differ from the behavior seen in most other viscoelastic materials, such as polymers, whose rheology can be described by physical models that predict universal exponents having specific numerical values independent of formulation details (104). It has been shown that critical gels (105), polymer gels near the mechanical percolation transition, also show power-law rheology with nonuniversal exponents. Critical gels are not classified as SGMs however, as their power-law rheology behaviors are only manifest in a narrow, engineered degree of cross-linking, unlike the robust behavior of SGMs.

Many SGMs (e.g., pastes and colloidal glasses) display physical aging and rejuvenation phenomena (106), wherein the measured linear rheology is time dependent, generally stiffening as a function of sample age, but able to return to early time behavior with modest shearing (93, 107). Such time dependence definitively indicates that these materials are nonergodic or glassy—they do not occupy or ever reach a global thermodynamic equilibrium state. SGMs that do not display such aging (e.g., foams and some emulsions) typically have high values of  $\beta$  and have internal rearrangements driven by coarsening and coalescence. It is generally supposed that the internal motions place the material in a state of continuous rejuvenation, creating a nonequilibrium, dynamical steady state. Lastly, still other SGMs (gels and clay suspensions) display even more complex and diverse aging behavior (96, 108).

**3.2.1. Theoretical models.** Early models to describe SGMs, including the soft glassy rheology (SGR) model (98, 99, 109) based on trap models of the glass transition (110), and a

second model based on MCT (111) were formulated in the late 1990s. More recently, the SGR model has been generalized to more complicated structures (112) and further refined (113). Both models capture many features of SGM phenomena (114, 115), with notable discrepancies (116).

**3.2.2. Cells.** Fredberg and coworkers (43) found that living cells' linear shear moduli have a weak power-law frequency dependence, with a (nonuniversal) exponent that varied among cell types and in response to treatments. They noted that the SGR model provided an excellent description and proposed that cells be considered SGMs. Other reports of SGM-type behavior in cells followed (117, 118), including non-Brownian fluctuations (58, 59), dynamical heterogeneity, aging, and rejuvenation (119).

**3.2.3. Summary and future directions.** Perhaps the biggest open question in the SGM field is whether the diverse phenomena of all SGMs can be described by a single model, or equivalently, whether the broad SGM phenomenological umbrella has lumped together materials whose rheologies, although similar, have deeply different physical origins. It is clear from the rheology that all materials highlighted above share common structural relaxation processes having a very broad (and nearly flat) spectrum of relaxation rates. It is also clear that most, if not all, of those relaxation processes are not thermally activated. Indeed, the nature and microscopic description of the activation processes in different SGMs are either known poorly or not at all. Thus, the second major focus in the SGM field is to understand the nature of the nonthermal activation in different materials, which is generally considered to have a Kramers-like form driven by an effective temperature (99), but which may have a different form and origin.

### 3.3. Granular Materials

Granular materials are conglomerates of athermal particles that interact via contact forces and can form jammed, solid-like states that resist shear (67, 68). The full gamut of granular static and dynamic phenomena includes regimes analogous to those of conventional solids, fluids, and gases, but also regimes that differ in fundamental ways (120). Understanding the behavior of granular materials is of importance for industry (e.g., storage in silos, transport, chemical processing in fluidized beds), energy (e.g., drilling through sand for oil recovery), and geophysical processes (e.g., earthquakes, dune formation).

For granular materials to flow, shear forces must be applied to overcome repulsive and frictional contact forces that maintain the particles' static configuration. This energy injection, or fluidization, is most commonly accomplished via shearing at the sample boundaries, via mechanical vibration of the boundaries, or by forcing air through the medium. In steady state, energy must be continuously injected into the system and is dissipated via inelastic interparticle interactions. Thus, granular dynamics are an intrinsically non-equilibrium phenomenon. In a steady state, a granular temperature is defined in terms of the root-mean-square velocity fluctuations of the particles. Experiments have been carried out to test whether classical equilibrium statistical mechanical relationships such as equipartition (121) and the FDT (122–124) are obeyed in fluidized granular media, albeit with the new granular temperature. Although many such experiments have been found to be in accord with an effective temperature picture (125, 126), its universality remains an open question. For example, in contrast to thermal systems, energy is almost always

injected anisotropically into a granular medium and is transferred heterogeneously down to the particle scale, due to the interplay of dissipative, gravitational, and boundary effects. These effects complicate, but also enrich, the dynamics of granular systems, and they must be carefully considered in the interpretation of experiments geared toward establishing parallels between granular and thermal systems.

Theories about the rheology of granular materials are challenging, in part due to the effects of inhomogeneity in force transmission. In contrast to continuous media such as Newtonian fluids, forces applied to granular media are almost always resisted inhomogeneously and anisotropically, e.g., by force chains comprised of only a very small fraction of the total number of particles (127–129). To date, the most striking demonstration of the existence of force chains has been observed in two-dimensional (2D) granular packings of disks. In this case, the force chains are observed via compaction of photoelastic disks that transmit light between crossed polarizers in extinction mode when stressed (130, 131). Qualitatively similar behavior of force chains has been observed in experiments wherein photoelastic disks were slowly sheared in a 2D Couette geometry (132). Thus, the motion of an immersed object through a granular medium requires breaking and reformation of force chains, resulting in temporally intermittent, stick-slip dynamics (133). The applicability of conventional continuum elastic/fluidic theory to these physical systems is clearly no longer apparent.

Granular rheology in 3D holds the most relevance for industrial application. Unfortunately, it is often not enough to simply measure stress as a function of shear rate in a rheometer, as in conventional fluids; additional information from, for example, simultaneous imaging of the granular microstructure in both the bulk and near the surfaces is necessary. To this end, experiments using magnetic resonance imaging (134) and internal optical imaging using index-matched grains/fluid (135) have been used to visualize internal granular microstructure under shear in a 3D annular volume. In both such experiments, shear banding behavior was generally observed wherein particles ordered into layers near the shearing wall.

### 3.4. Cross-Linked Networks

Polymer networks are rich in mechanical properties, which can be modulated by varying the nature of the polymers, cross-linking agents, and the interactions between polymers. In a cross-linked network, polymers are linked together by permanent bonds that prevent relative motions of the polymers. The cross-linkers can be covalent bonds between polymers, can be an individual molecule that can bind to multiple filaments, or can be branch points from a larger fiber in the network. For the most part, the rheological properties of cross-linked flexible polymers such as rubber are well described by classical theories of rubber elasticity (136), wherein polymer strands between cross-links are treated as springs whose elastic response under stretching or compression is derived from the entropic cost of the polymer strand's reduced conformational degrees of freedom. Cross-linked networks are different from entangled networks, which are held together only by physical entanglement between polymers. Most notably, entangled networks possess mechanisms of stress relaxation that are absent in cross-linked networks. The most important of these mechanisms is reptation, in which stress relaxation occurs via polymer diffusion in a tube formed by its neighbors (104). Reptation sets a characteristic frequency below which entangled networks exhibit a linear viscoelastic response that is dominantly liquid-like ( $G'' > G'$ ).

In cross-linked networks, this regime is absent because cross-linking prevents reptation (and hence stress relaxation), leading to a dominantly elastic ( $G' > G''$ ) response. Above the reptation frequency, entangled and cross-linked networks are hard to distinguish rheologically. At an intermediate frequency range, often referred to as the rubber plateau, both networks exhibit a frequency-independent elastic modulus. At frequencies above the rubber plateau, both networks exhibit power-law frequency dependence with exponents characteristic of single polymer responses.

Polymer theory distinguishes three types of filaments according to the ratio between persistence length ( $l_p$ ) and contour length ( $l_c$ ). The persistence length is defined as the length scale for the decay of the tangent-tangent correlation along the filament contour, and it is proportional to the stiffness of the polymer chain. When  $l_c \gg l_p$ , the filament is considered to be soft and exhibit purely entropic elastic response. In the limit of  $l_p \gg l_c$ , filaments are stiff and show no entropic elasticity. Most biopolymers fall between these two limits—they are semiflexible with  $l_c$  and  $l_p$  approximately the same order of magnitude. Currently, the properties of semiflexible polymer networks have been intensively investigated due to their biological relevance. Microscopic properties of the network deformations such as the deformation of individual polymers and the distribution of deformation fields in the network must be understood to explain the mechanical properties of these biopolymer networks. Unique properties such as negative normal stress (137) and strain stiffening at moderate strain amplitudes (2) have been recently observed in these biopolymer networks and have spurred the development of theories describing semiflexible networks.

**3.4.1. Nonlinear elasticity of biological polymers.** For gels of flexible polymers such as polyacrylamide,  $G'$  is a constant for strain values up to 100%: The flexible polymer responds linearly. In contrast, gels of actin, fibrin, and collagen show strain stiffening behavior at medium strain levels, i.e., the  $G'$  of these gels becomes larger at larger strains. A small increase ( $< 20\%$ ) in shear strain can lead to tenfold (or more) increase in shear elastic moduli (2).

The origin of strain stiffening in networks of semiflexible or rod-like polymers has been addressed by several recent theories. For filaments that are highly elongated but still soft enough to be deformed by thermal energy, for example, polymers with persistence length on the order of the network mesh size, nonlinear strain stiffening occurs as a result of the intrinsically nonlinear force-extension relation of each network strand (2, 138). If the persistence length of the filament is comparable to the mesh size or distance between cross-links within the network, then strain stiffening emerges from an entropic model that considers how thermal fluctuations of semiflexible polymers are constrained as the end-to-end distance of filament segments between cross-links changes when the sample is deformed (2, 5, 138, 139). This essentially entropic model accurately predicts the strain-dependent elasticity of isotropically cross-linked F-actin, intermediate filaments, and fibrin protofibrils, which have persistence lengths between 0.5 and 10 microns and form networks with mesh size on the order of 100 nm to 1 micron (2). Other networks formed by much stiffer and thicker fibers, such as collagen, fibrin fibers, or actin bundles also exhibit strain stiffening, but the degree of strain stiffening appears to be less than that of the intermediate filaments, and thermal motions of these stiffer fibers would appear not to play a significant role in their response. In these cases, models derived from the enthalpic deformation of soft rods have been developed. In these models, strain stiffening coincides

with alignment of fibers in the strain direction and a shift from soft bending modes to stiffer stretching modes as the fibers reorient (140–143)

**3.4.2. Normal stress.** A novel feature of semiflexible network rheology is that deformations that are pure shear lead to a negative normal stress that tends to pull the shearing surfaces toward each other. When cross-linked networks of F-actin, fibrin, collagen, or other biopolymers are sheared, the stress directed orthogonal to the strain direction increases quadratically with shear strain and can have a magnitude close to that of the shear stress (1, 137). Flexible polymer gels generally have negligible normal stress, and at high strains exhibit a positive normal stress that is much smaller than the shear stress, in accord with predictions of the Mooney-Rivlin theory of rubber elasticity (136). Negative normal stress emerges naturally from the thermal model for semiflexible filaments. The force-displacement relation for such filaments shows that less force is needed to compress such a filament than to stretch it, and, therefore, under pure shear the downward-directed forces from stretched filaments oriented away from the shear direction dominate over the weaker upward-directed forces from the compressed filaments (1, 137). Nonthermal models of stiff filaments also predict negative normal stress, because compressed filaments can buckle and thus reduce upward forces relative to the always increased downward forces produced by stretched filaments (144). Some models predict that the normal stresses can be even greater than shear stresses under some conditions (145).

**3.4.3. Affine versus nonaffine deformation.** One important assumption in theories of rubber elasticity and entropic models for elasticity of networks of semiflexible polymers is that the macroscopic network deformation is transferred uniformly to each polymer chain in the network. Various theories developed for the rheology of stiff or semiflexible networks make different predictions about the degree to which the deformations are affine, that is, the degree to which local strains match the macroscopic strain, and about the extent to which filament alignment occurs. Direct measurement of network nonaffinity, made by quantifying the displacement of small markers placed within the network, have begun to differentiate between these different theoretical models, and more fully define the material response in these networks (11, 142, 146, 147). As the polymer stiffness increases, transverse thermal undulation of polymers is negligible and the elasticity of filaments is no longer entropic. For example, in a bundled actin network, the deformation is dominated by nonaffine enthalpic bending of the actin bundles (5, 148). Computer simulations suggest that the nonaffine deformation of gels made of rigid filaments is accompanied by filament bending, rotation, and buckling (149).

Nonaffine deformation occurs not only in stiff polymer networks but also in semiflexible and even flexible polymer networks. In random elastic media, heterogeneities in local elasticity can give rise to nonaffine deformations (150). In semiflexible polymer networks, nonaffine deformations have been measured for actin gels (16) and fibrin gels (11), by measuring displacements of tracer beads in the gels under external stress.

**3.4.4. Active gels.** The cytoskeleton of a cell is composed of filamentous actin network and different types of molecular motors actively moving along the actin filaments and applying forces to the filament. An active gel often refers to filament networks containing molecular motors. Many cell functions, including but not limited to cell migration, mechanosensing, and adaptation to environments, are related to the dynamics and

rheological properties of the cytoskeleton (151). A recent study on purified actin networks cross-linked by filamin shows that adding myosin II motors leads to an increase in  $G'$  by more than two orders of magnitude. This suggests that one function of myosin II is to pull the actin filaments and cause an internal stress that stiffens the cytoskeleton (152). The strain stiffening of cross-linked actin networks in combination with the myosin motors allow cells to adjust their cortical stiffness by modulating the motor activity. This effect provides a possible explanation for a recent cell mechanosensing observation that fibroblasts can adjust their stiffness to match the stiffness of the substrates they are cultured on (153).

**3.4.5. Summary and future directions.** Nonlinear elasticity, negative normal stress, and nonaffine deformations are signatures of semiflexible polymer networks. The available theoretical models on elasticity of semiflexible polymer networks are derived from two different origins: the affine entropy model and the nonaffine enthalpy model. The former model suggests these effects originate from entropic stretching of thermal fluctuations, whereas the latter suggests an origin in bending and buckling of soft rods. Although both are able to predict the onset and extent of these effects on a coarse-grained level, experimental techniques capable of monitoring single filament/bundle dynamics under shear, such as confocal rheometry, are needed to decisively distinguish between these alternative models.

The current research approach of examining *in vitro* isotropic networks under well-defined shear deformations has been very successful in elucidating the physical properties of semiflexible networks. However, *in vivo* networks rarely exist and operate under such ideal conditions. Often, functional cellular networks are composed of different types of filaments and cross-linking proteins, possess some degree of anisotropy, and are quasi-2D. Future work in the field will no doubt be oriented toward exploring these complexities both experimentally and theoretically.

In a related vein, asking the question of why Nature decided to utilize certain classes of network constituents (e.g., semiflexible, active molecular motors) to accomplish crucial biological functions will continue to drive future research on polymer networks. One promising approach, multiscale mechanics, aims to uncover such underlying design principles by investigating dynamics from the single-molecule, to filament, to network scales. An exciting example of multiscale mechanics can be found in recent work on networks of the blood-clotting protein fibrin. The authors relate the consequences of unfolding of the fibrin proteins at the single-molecule scale to functional requirements of permeability and extensibility at the clot scale (154).

### 3.5. Cells

Viewed as a soft material, the cell is arguably the most challenging to characterize and interpret of all the soft materials reviewed here. The complexity arises in large part from there being a variety of load-bearing elements and heterogeneous substructures inside cells. These elements and structures are coupled mechanically through both passive (mechanical) and active (ATP-dependent) processes and have multiple timescales of response. Additionally, most cells contain endogenous molecular force sensors that trigger biochemical signaling pathways that may modulate cellular stiffness in response to shear forces with specific characteristics, a process known as mechanosensing. Although important to the comprehensive picture of cell mechanics, consideration of the mechanisms of

mechanosensing are beyond the scope of the present work and are reviewed in detail elsewhere (155, 156). Instead, we focus on soft material aspects of cells' rheological responses, in essence, viewing the cell as an exotic, hierarchically structured, soft material.

When probed, cells' rheological behavior shares many characteristics of nearly every class of soft material reviewed here. Cells exhibit linear viscoelastic moduli with scaling exponents characteristic of stress relaxation in semiflexible polymer networks. This is not too surprising because actin, microtubules, and intermediate filaments comprise a large part of the cytoskeleton, nucleus, and cortex of mammalian cells. Also, many studies have shown that cells exhibit strain stiffening in response to stress or deformation (157). The precise origins of the strain-stiffening response of cells is not fully understood and may reflect, in addition to orientation, alignment, and the pulling out of entropic fluctuations under shear, an important contribution from prestress due to active elements such as molecular motors (60, 158, 159). Under physiological conditions, cells are subject to highly nonlinear strains of both externally and internally generated origins. The assumption that information relevant to cell mechanics *in vivo* can be learned from its linear viscoelastic properties, as in simple materials, is thus called into question.

Cells are internally quite crowded, and thus cells share with dense colloidal glasses, SGMs, and granular materials the property that they are jammed in a metastable, nonergodic state and require rejuvenation via internally generated nonthermal forces to rearrange, *i.e.*, to move or divide in the case of cells. Indeed, concepts from the theory of soft glassy rheology (SGR) (98), such as aging and shear rejuvenation, have been adapted to interpret cell rheology experiments (43, 119, 160). Similar to SGMs, cells have power-law rheology in which the modulus increases slowly with a nonuniversal weak exponent even at low frequency (43). In contrast, biopolymer networks with comparable elastic moduli (100–1000 Pa) would be purely elastic, exhibiting a frequency-independent plateau modulus at low frequencies. There are, however, notable differences between cell and SGM rheology (161). For one, the observation of strain stiffening in some cell studies (157) is inconsistent with SGM rheology, which generally exhibits yielding and plasticity, as observed in cell softening seen under large oscillatory strain (119). Of course, multiple explanations are possible: the stiffening could be due to a background network that is pervaded by an SGM or conversely, the cell softening and subsequent aging could be due to mechanical network damage and active repair (119). If the non-Brownian fluctuations in cells are responsible for SGM-like fluidization, then the observed rheology exponent should be very sensitive to ATP perturbation, which it is not (119, 162). The original, nonuniversal exponent findings can also be explained as resulting from the superposition of multiple structures having different rheology (161).

In the face of the daunting complexity of a cell's rheological response, two main approaches have been undertaken. The first is a bottom-up approach in which the constituents of a cell are extracted, purified, reconstituted, and used to create a minimal *in vitro* system capable of faithfully replicating an intact cell's rheological feature of interest. Cells, after all, are comprised primarily of biopolymers; thus, by starting with a reconstituted network with a well-understood rheological response, it follows that one might be able to serially build up the complexity by adding cross-linking proteins, active molecular motors, *etc.* Notable successes of this approach include replication of strain-stiffening behavior using prestressed flexible cross-linking proteins (163) and molecular motors (60) in reconstituted actin networks. Alternatively, a top-down approach has been undertaken in which whole, functioning cells are probed using microrheological techniques covering a

**Table 1** Summary matrix of soft material classes and observed rheological effects. (X denotes observation of effect and reference.)

	Power-law rheology	Shear thinning/ strain softening	Shear thickening/ strain stiffening	Shear banding	Active (nonequilibrium) effects	Aging after shear rejuvenation/ fluidization
Colloidal suspensions	X (69)	X (75)	X (75)	X (15)	X (47)	
Colloidal glasses	X (69)	X (87)		X (87)		X (106)
Granular materials			X (132)	X (135)	X (122)	X (124)
Soft glassy materials	X (91)	X (91)		X (14)	X (99)	X (108)
Polymer networks	X (105)		X (2)	X (10)	X (60)	
Cells	X (43)	X (119)	X (157)		X (59)	X (119)

wide range of intracellular length and timescales in concert with pharmacological interventions designed to eliminate mutually confounding response pathways. The emergent principal components of the data are usually in the form of scaling exponents characterizing frequency-dependent rheological response functions. These functions are then used to formulate a consensus description. Notable successes of this approach include the discoveries of distinct power laws characterizing the rheological responses of the deep cell interior and outer cortex (162). This approach is reviewed in Reference 161.

## 4. CONCLUSIONS AND OUTLOOK

### SUMMARY POINTS

1. Rheology and microrheology are chief ways of probing the structure and responses of soft materials.
2. The linear response of soft materials is typically described by complex frequency-dependent shear moduli that encode information about the underlying structures and timescales of the material. It is hard to distinguish soft materials from each other based only on their linear viscoelastic moduli.
3. When driven to nonlinear strain regimes (polymeric materials), or out of equilibrium at high shear rates (colloidal suspensions), soft materials exhibit a wide range of striking and technologically useful responses (e.g., shear thinning/thickening, shear banding).
4. Many classes of soft materials, although constitutively distinct, exhibit rheological properties that can be captured by a small set of phenomenological models such as SGR, jamming, and polymer rheology (Table 1).

## FUTURE ISSUES

1. Current trends to simultaneously image and shear materials (e.g., confocal rheometry) promise to reveal a mechanistic understanding of soft material deformation at an unprecedented level of detail. This bodes well for guiding the development of theoretical models and suggesting new technological applications.
2. One ultimate test of our understanding of soft material rheology lies in our ability to predict the rheological responses of cells, for which a comprehensive, multiscale approach integrating all aspects of soft materials rheology must be brought to bear.

## DISCLOSURE STATEMENT

The authors are not aware of any affiliations, memberships, funding, or financial holdings that might be perceived as affecting the objectivity of this review.

## ACKNOWLEDGMENTS

We gratefully acknowledge useful discussions over many years with Tom Lubensky, Fred MacKintosh, Andrea Liu, Doug Durian, Jerry Gollub, Eric Weeks, Alex Levine, Andy Lau, Ke Chen, Ahmed Alsayed, Anindita Basu, Zexin Zhang, Larry Hough, Mohammad Islam, and Peter Yunker. A.G.Y. acknowledges support from NSF-MRSEC (DMR-0505048), NSF (DMR 05-20020), and NASA (NNX08AO0G). J.C.C. acknowledges support from the NSF (DMR-0706388). P.A.J. acknowledges support from NIH (GM083272).

## LITERATURE CITED

1. Kang H, Wen Q, Janmey PA, Tang JX, Conti E, MacKintosh FC. 2009. *J. Phys. Chem. B* 113:3799–805
2. Storm C, Pastore JJ, MacKintosh FC, Lubensky TC, Janmey PA. 2005. *Nature* 435:191–94
3. Schopferer M, Bar H, Hochstein B, Sharma S, Mucke N, et al. 2009. *J. Mol. Biol.* 388:133–43
4. Gardel ML, Nakamura F, Hartwig J, Crocker JC, Stossel TP, Weitz DA. 2006. *Phys. Rev. Lett.* 96:088102
5. Gardel ML, Shin JH, MacKintosh FC, Mahadevan L, Matsudaira P, Weitz DA. 2004. *Science* 304:1301–5
6. Kasza KE, Koenderink GH, Lin YC, Broedersz CP, Messner W, et al. 2009. *Phys. Rev. E* 79:041928
7. Ewoldt RH, Hosoi AE, McKinley GH. 2008. *J. Rheol.* 52:1427–58
8. Fielding SM. 2007. *Soft Matter* 3:1262–79
9. Olmsted PD. 2008. *Rheol. Acta* 47:283–300
10. Boukany PE, Hu YT, Wang SQ. 2008. *Macromolecules* 41:2644–50
11. Wen Q, Basu A, Winer JP, Yodh A, Janmey PA. 2007. *New J. Phys.* 9:428
12. Besseling R, Isa L, Weeks ER, Poon WCK. 2009. *Adv. Colloid Interface Sci.* 146:1–17
13. Callaghan PT. 2008. *Rheol. Acta* 47:243–55

14. Coussot P, Raynaud JS, Bertrand F, Moucheron P, Guilbaud JP, et al. 2002. *Phys. Rev. Lett.* 88:218301
15. Cohen I, Davidovitch B, Schofield AB, Brenner MP, Weitz DA. 2006. *Phys. Rev. Lett.* 97:215502
16. Liu J, Koenderink GH, Kasza KE, MacKintosh FC, Weitz DA. 2007. *Phys. Rev. Lett.* 98:198304
17. Vermant J, Solomon MJ. 2005. *J. Phys. Condens. Matter* 17:R187–216
18. Wagner NJ. 1998. *Curr. Opin. Colloid Interface Sci.* 3:391–400
19. Seifriz W. 1924. *J. Exp. Biol.* 2:1–11
20. Crick FHC, Hughes AFW. 1950. *Exp. Cell Res.* 1:37–80
21. Mason TG, Gang H, Weitz DA. 1997. *J. Opt. Soc. Am. A* 14:139–49
22. Gittes F, Schnurr B, Olmsted PD, MacKintosh FC, Schmidt CF. 1997. *Phys. Rev. Lett.* 79:3286–89
23. Mason TG, Ganesan K, van Zanten JH, Wirtz D, Kuo SC. 1997. *Phys. Rev. Lett.* 79:3282–85
24. Starrs L, Bartlett P. 2003. *J. Phys. Condens. Matter* 15:S251–56
25. Addas KM, Schmidt CF, Tang JX. 2004. *Phys. Rev. E* 70:021503
26. Palmer A, Mason TG, Xu JY, Kuo SC, Wirtz D. 1999. *Biophys. J.* 76:1063–71
27. Gisler T, Weitz DA. 1999. *Phys. Rev. Lett.* 82:1606–9
28. Dasgupta BR, Tee SY, Crocker JC, Frisken BJ, Weitz DA. 2002. *Phys. Rev. E* 65:051505
29. Popescu G, Dogariu A, Rajagopalan R. 2002. *Phys. Rev. E* 65:041504
30. Valentine MT, Perlman ZE, Gardel ML, Shin JH, Matsudaira P, et al. 2004. *Biophys. J.* 86:4004–14
31. Crocker JC, Valentine MT, Weeks ER, Gisler T, Kaplan PD, et al. 2000. *Phys. Rev. Lett.* 85:888–91
32. Chen DT, Weeks ER, Crocker JC, Islam MF, Verma R, et al. 2003. *Phys. Rev. Lett.* 90:108301
33. Popescu G, Park Y, Lue N, Best-Popescu C, Deflores L, et al. 2008. *Am. J. Physiol. Cell Physiol.* 295:C538–44
34. Benmouna F, Johannsmann D. 2004. *Langmuir* 20:188–93
35. Habdas P, Schaar D, Levitt AC, Weeks ER. 2004. *Europhys. Lett.* 67:477–83
36. Squires TM. 2008. *Langmuir* 24:1147–59
37. Sriram I, Furst EM, DePuit RJ, Squires TM. 2009. *J. Rheol.* 53:357–81
38. White JG, Burris SM, Tukey D, Smith C, Clawson CC. 1984. *Blood* 64:210–14
39. Lerche D, Kozlov MM, Meier W. 1991. *Eur. Biophys. J.* 19:301–9
40. Discher DE, Mohandas N, Evans EA. 1994. *Science* 266:1032–35
41. Bausch AR, Hellner U, Essler M, Aepfelbacher M, Sackmann E. 2001. *Biophys. J.* 80:2649–57
42. Ziemann F, Radler J, Sackmann E. 1994. *Biophys. J.* 66:2210–16
43. Fabry B, Maksym GN, Butler JP, Glogauer M, Navajas D, Fredberg JJ. 2001. *Phys. Rev. Lett.* 87:148102
44. Puig-de-Morales M, Grabulosa M, Alcaraz J, Mullol J, Maksym GN, et al. 2001. *J. Appl. Physiol.* 91:1152–59
45. Mizuno D, Head DA, MacKintosh FC, Schmidt CF. 2008. *Macromolecules* 41:7194–202
46. Hough LA, Ou-Yang HD. 2006. *Phys. Rev. E* 73:031802
47. Chen DTN, Lau AWC, Hough LA, Islam MF, Goulian M, et al. 2007. *Phys. Rev. Lett.* 99:148302
48. Mahaffy RE, Shih CK, MacKintosh FC, Kas J. 2000. *Phys. Rev. Lett.* 85:880–83
49. Chaudhuri O, Parekh SH, Fletcher DA. 2007. *Nature* 445:295–98
50. Schmidt FG, Ziemann F, Sackmann E. 1996. *Eur. Biophys. J.* 24:348–53
51. Levine AJ, Lubensky TC. 2000. *Phys. Rev. Lett.* 85:1774–77
52. Levine AJ, Lubensky TC. 2001. *Phys. Rev. E* 65:011501
53. Atakhorrami M, Koenderink GH, Schmidt CF, MacKintosh FC. 2005. *Phys. Rev. Lett.* 95:208302
54. Qiu XL, Tong P, Ackerson BJ. 2004. *Appl. Opt.* 43:3382–90

55. Koenderink GH, Atakhorrami M, MacKintosh FC, Schmidt CF. 2006. *Phys. Rev. Lett.* 96:138307
56. Caspi A, Granek R, Elbaum M. 2002. *Phys. Rev. E* 66:011916
57. Salman H, Gil Y, Granek R, Elbaum M. 2002. *Chem. Phys.* 284:389–97
58. Bursac P, Fabry B, Trepap X, Lenormand G, Butler JP, et al. 2007. *Biochem. Biophys. Res. Commun.* 355:324–30
59. Lau AWC, Hoffman BD, Davies A, Crocker JC, Lubensky TC. 2003. *Phys. Rev. Lett.* 91:198101
60. Mizuno D, Tardin C, Schmidt CF, MacKintosh FC. 2007. *Science* 315:370–73
61. Brangwynne CP, Koenderink GH, MacKintosh FC, Weitz DA. 2008. *J. Cell Biol.* 183:583–87
62. Gallet F, Arcizet D, Bohec P, Richert A. 2009. *Soft Matter* 5:2947–53
63. Zhang Z, Xu N, Chen DTN, Yunker P, Alsayed AM, et al. 2009. *Nature* 459:230–33
64. Einstein A. 1905. *Ann. Phys.* 17:549–60
65. Batchelor GK, Green JT. 1972. *J. Fluid Mech.* 56:401–27
66. Bergenholtz J. 2001. *Curr. Opin. Colloid Interface Sci.* 6:484–88
67. Liu AJ, Nagel SR. 1998. *Nature* 396:21–22
68. Cates ME, Wittmer JP, Bouchaud JP, Claudin P. 1998. *Phys. Rev. Lett.* 81:1841–44
69. Mason TG, Weitz DA. 1995. *Phys. Rev. Lett.* 75:2770–73
70. Cheng ZD, Zhu JX, Chaikin PM, Phan SE, Russel WB. 2002. *Phys. Rev. E* 65:041405
71. Shikata T, Pearson DS. 1994. *J. Rheol.* 38:601–16
72. Brambilla G, El Masri D, Pierno M, Berthier L, Cipelletti L, et al. 2009. *Phys. Rev. Lett.* 102:085703
73. Gotze W, Sjogren L. 1992. *Rep. Prog. Phys.* 55:241–376
74. Turnbull D, Cohen MH. 1970. *J. Chem. Phys.* 52:3038
75. Maranzano BJ, Wagner NJ. 2001. *J. Chem. Phys.* 114:10514–27
76. Wagner NJ, Brady JF. 2009. *Phys. Today* 62:27–32
77. Hatwalne Y, Ramaswamy S, Rao M, Simha RA. 2004. *Phys. Rev. Lett.* 92:118101
78. Lau AWC, Lubensky TC. 2009. *Phys. Rev. E* 80:011917
79. Wu XL, Libchaber A. 2000. *Phys. Rev. Lett.* 84:3017–20
80. Dombrowski C, Cisneros L, Chatkaew S, Goldstein RE, Kessler JO. 2004. *Phys. Rev. Lett.* 93:098103
81. Sokolov A, Aranson IS. 2009. *Phys. Rev. Lett.* 103:148101
82. Weeks ER, Crocker JC, Levitt AC, Schofield A, Weitz DA. 2000. *Science* 287:627–31
83. Kegel WK, van Blaaderen A. 2000. *Science* 287:290–93
84. Yunker P, Zhang Z, Aptowicz KB, Yodh AG. 2009. *Phys. Rev. Lett.* 103:115701
85. Langer JS. 2008. *Phys. Rev. E* 77:021502
86. Schall P, Weitz DA, Spaepen F. 2007. *Science* 318:1895–99
87. Besseling R, Weeks ER, Schofield AB, Poon WCK. 2007. *Phys. Rev. Lett.* 99:028301
88. Lynch JM, Cianci GC, Weeks ER. 2008. *Phys. Rev. E* 78:031410
89. Cloitre M, Borrega R, Monti F, Leibler L. 2003. *Phys. Rev. Lett.* 90:068303
90. Hohler R, Cohen-Addad S. 2005. *J. Phys. Condens. Matter* 17:R1041–69
91. Mason TG, Bibette J, Weitz DA. 1995. *Phys. Rev. Lett.* 75:2051–54
92. Becu L, Manneville S, Colin A. 2006. *Phys. Rev. Lett.* 96:138302
93. Courtland RE, Weeks ER. 2003. *J. Phys. Condens. Matter* 15:S359–65
94. Treece MA, Oberhauser JP. 2007. *Polymer* 48:1083–95
95. Christopoulou C, Petekidis G, Erwin B, Cloitre M, Vlassopoulos D. 2009. *Philos. Trans. R. Soc. Ser. 367*: 5051–71
96. Ramos L, Cipelletti L. 2001. *Phys. Rev. Lett.* 87:245503
97. Barnes HA, Hutton JF, Walters K. 2001. *An Introduction to Rheology*. Amsterdam: Elsevier Sci.
98. Sollich P, Lequeux F, Hebraud P, Cates ME. 1997. *Phys. Rev. Lett.* 78:2020–23
99. Sollich P. 1998. *Phys. Rev. E* 58:738–59

100. Conrad JC, Lewis JA. 2008. *Langmuir* 24:7628–34
101. Gibaud T, Barentin C, Taberlet N, Manneville S. 2009. *Soft Matter* 5:3026–37
102. Ianni F, Di Leonardo R, Gentilini S, Ruocco G. 2008. *Phys. Rev. E* 77:031406
103. Moller PCF, Rodts S, Michels MAJ, Bonn D. 2008. *Phys. Rev. E* 77:041507
104. Doi M, Edwards SF. 1986. *The Theory of Polymer Dynamics*. New York: Oxford Univ. Press
105. Izuka A, Winter H, Hashimoto T. 1992. *Macromolecules* 25:2422–28
106. Moller P, Fall A, Chikkadi V, Derks D, Bonn D. 2009. *Philos. Trans. R. Soc. Ser. A* 367:5139–55
107. McKenna GB, Narita T, Lequeux F. 2009. *J. Rheol.* 53:489–516
108. Ianni F, Di Leonardo R, Gentilini S, Ruocco G. 2007. *Phys. Rev. E* 75:011408
109. Fielding SM, Sollich P, Cates ME. 2000. *J. Rheol.* 44:323–69
110. Bouchaud JP. 1992. *J. Phys. I* 2:1705–13
111. Hebraud P, Lequeux F. 1998. *Phys. Rev. Lett.* 81:2934–37
112. Cates ME, Sollich P. 2004. *J. Rheol.* 48:193–207
113. Fielding SM, Cates ME, Sollich P. 2009. *Soft Matter* 5:2378–82
114. Helgeson ME, Wagner NJ, Vlassopoulos D. 2007. *J. Rheol.* 51:297–316
115. Purnomo EH, van den Ende D, Mellema J, Mugele F. 2007. *Phys. Rev. E* 76:021404
116. Yin GJ, Solomon MJ. 2008. *J. Rheol.* 52:785–800
117. Mofrad MRK. 2009. *Annu. Rev. Fluid Mech.* 41:433–53
118. Smith BA, Roy H, De Koninck P, Grutter P, De Koninck Y. 2007. *Biophys. J.* 92:1419–30
119. Bursac P, Lenormand G, Fabry B, Oliver M, Weitz DA, et al. 2005. *Nat. Mater.* 4:557–61
120. Jaeger HM, Nagel SR, Behringer RP. 1996. *Rev. Mod. Phys.* 68:1259–73
121. Feitosa K, Menon N. 2002. *Phys. Rev. Lett.* 88:198301
122. D'Anna G, Mayor P, Barrat A, Loreto V, Nori F. 2003. *Nature* 424:909–12
123. Ojha RP, Lemieux PA, Dixon PK, Liu AJ, Durian DJ. 2004. *Nature* 427:521–23
124. Jossierand C, Tkachenko AV, Mueth DM, Jaeger HM. 2000. *Phys. Rev. Lett.* 85:3632–35
125. Corwin EI, Jaeger HM, Nagel SR. 2005. *Nature* 435:1075–78
126. Song C, Wang P, Makse HA. 2005. *Proc. Natl. Acad. Sci. USA* 102:2299–304
127. Liu CH, Nagel SR, Schecter DA, Coppersmith SN, Majumdar S, et al. 1995. *Science* 269:513–15
128. Dantu P. 1968. *Geotechnique* 18:50
129. Travers T, Bideau D, Gervois A, Troadec JP, Messenger JC. 1986. *J. Phys. A* 19:1033–38
130. Howell D, Behringer RP, Veje C. 1999. *Phys. Rev. Lett.* 82:5241–44
131. Drescher A, de Josselin de Jong G. 1972. *J. Mech. Phys. Solids* 20:337
132. Hartley RR, Behringer RP. 2003. *Nature* 421:928–31
133. Albert I, Tegzes P, Kahng B, Albert R, Sample JG, et al. 2000. *Phys. Rev. Lett.* 84:5122–25
134. Mueth DM, Debregeas GF, Karczmar GS, Eng PJ, Nagel SR, Jaeger HM. 2000. *Nature* 406:385–89
135. Tsai JC, Voth GA, Gollub JP. 2003. *Phys. Rev. Lett.* 91:064301
136. Rubinstein M, Colby RH. 2003. *Polymer Physics*. Oxford/New York: Oxford Univ. Press. xi. 440 pp.
137. Janmey PA, McCormick ME, Rammensee S, Leight JL, Georges PC, MacKintosh FC. 2007. *Nat. Mater.* 6:48–51
138. MacKintosh FC, Kas J, Janmey PA. 1995. *Phys. Rev. Lett.* 75:4425–28
139. Palmer JS, Boyce MC. 2008. *Acta Biomater.* 4:597–612
140. Huisman EM, van Dillen T, Onck PR, van der Giessen E. 2007. *Phys. Rev. Lett.* 99:208103
141. Onck PR, Koeman T, van Dillen T, van der Giessen E. 2005. *Phys. Rev. Lett.* 95:178102
142. Heussinger C, Shaefer B, Frey E. 2007. *Phys. Rev. E* 76:031906
143. van Dillen T, Onck PR, van der Giessen E. 2008. *J. Mech. Phys. Solids* 56:2240–64
144. Conti E, MacKintosh FC. 2009. *Phys. Rev. Lett.* 102:088102
145. Heussinger C, Frey E. 2006. *Phys. Rev. Lett.* 97:105501
146. Fernandez P, Grosser S, Kroy K. 2009. *Soft Matter* 5:2047–56
147. Hatami-Marbini H, Picu RC. 2008. *Phys. Rev. E* 77:062103

148. Lieleg O, Claessens MM, Heussinger C, Frey E, Bausch AR. 2007. *Phys. Rev. Lett.* 99:088102
149. Chandran PL, Barocas VH. 2006. *J. Biomech. Eng.* 128:259–70
150. DiDonna BA, Lubensky TC. 2005. *Phys. Rev. E* 72:066619
151. Fletcher DA, Geissler PL. 2009. *Annu. Rev. Phys. Chem.* 60:469–86
152. Koenderink GH, Dogic Z, Nakamura F, Bendix PM, MacKintosh FC, et al. 2009. *Proc. Natl. Acad. Sci. USA* 106:15192–97
153. Solon J, Levental I, Sengupta K, Georges PC, Janmey PA. 2007. *Biophys. J.* 93:4453–61
154. Brown AEX, Litvinov RI, Discher DE, Purohit PK, Weisel JW. 2009. *Science* 325:741–44
155. Shyy JY, Chien S. 2002. *Circ. Res.* 91:769–75
156. Janmey PA, McCulloch CA. 2007. *Annu. Rev. Biomed. Eng.* 9:1–34
157. Wang N, Butler JP, Ingber DE. 1993. *Science* 260:1124–27
158. Brangwynne CP, Koenderink GH, MacKintosh FC, Weitz DA. 2008. *Phys. Rev. Lett.* 100:118104
159. Kumar S, Maxwell IZ, Heisterkamp A, Polte TR, Lele TP, et al. 2006. *Biophys. J.* 90:3762–73
160. Deng L, Treppe X, Butler JP, Millet E, Morgan KG, et al. 2006. *Nat. Mater.* 5:636–40
161. Hoffman BD, Crocker JC. 2009. *Annu. Rev. Biomed. Eng.* 11:259–88
162. Hoffman BD, Massiera G, Van Citters KM, Crocker JC. 2006. *Proc. Natl. Acad. Sci. USA* 103:10259–64
163. Gardel ML, Nakamura F, Hartwig JH, Crocker JC, Stossel TP, Weitz DA. 2006. *Proc. Natl. Acad. Sci. USA* 103:1762–67



# Contents

Electron Transport in Carbon Nanotubes <i>Shahal Ilani and Paul L. McEuen</i> . . . . .	1
FeAs-Based Superconductivity: A Case Study of the Effects of Transition Metal Doping on $\text{BaFe}_2\text{As}_2$ <i>Paul C. Canfield and Sergey L. Bud'ko</i> . . . . .	27
Scattering and Pairing in Cuprate Superconductors <i>Louis Taillefer</i> . . . . .	51
Spintronics <i>S.D. Bader and S.S.P. Parkin</i> . . . . .	71
Characterizing Graphene, Graphite, and Carbon Nanotubes by Raman Spectroscopy <i>M.S. Dresselhaus, A. Jorio, and R. Saito</i> . . . . .	89
Single-Molecule Nanomagnets <i>Jonathan R. Friedman and Myriam P. Sarachik</i> . . . . .	109
Fermi-Hubbard Physics with Atoms in an Optical Lattice <i>Tilman Esslinger</i> . . . . .	129
Nematic Fermi Fluids in Condensed Matter Physics <i>Eduardo Fradkin, Steven A. Kivelson, Michael J. Lawler, James P. Eisenstein, and Andrew P. Mackenzie</i> . . . . .	153
The “Coulomb Phase” in Frustrated Systems <i>Christopher L. Henley</i> . . . . .	179
First-Principles Calculations of Complex Metal-Oxide Materials <i>Karin M. Rabe</i> . . . . .	211
X-Ray Diffraction Microscopy <i>Pierre Thibault and Veit Elser</i> . . . . .	237

Physics of Cellular Movements <i>Erich Sackmann, Felix Keber, and Doris Heinrich</i> . . . . .	257
Molecular Theories of Segmental Dynamics and Mechanical Response in Deeply Supercooled Polymer Melts and Glasses <i>Kang Chen, Erica J. Saltzman, and Kenneth S. Schweizer</i> . . . . .	277
Rheology of Soft Materials <i>Daniel T.N. Chen, Qi Wen, Paul A. Janmey, John C. Crocker, and Arjun G. Yodh</i> . . . . .	301
The Mechanics and Statistics of Active Matter <i>Sriram Ramaswamy</i> . . . . .	323
The Jamming Transition and the Marginally Jammed Solid <i>Andrea J. Liu and Sidney R. Nagel</i> . . . . .	347
Dynamics of Simple Cracks <i>Eran Bouchbinder, Jay Fineberg, and M. Marder</i> . . . . .	371
Friction, Fracture, and Earthquakes <i>Eric G. Daub and Jean M. Carlson</i> . . . . .	397

**Errata**

An online log of corrections to *Annual Review of Condensed Matter Physics* articles may be found at <http://conmatphys.annualreviews.org/errata.shtml>